

Functional Selectivity of G Protein Signaling by Agonist Peptides and Thrombin for the Protease-activated Receptor-1*[§]

Received for publication, December 15, 2004, and in revised form, April 22, 2005
Published, JBC Papers in Press, May 4, 2005, DOI 10.1074/jbc.M414090200

Joseph N. McLaughlin, Lixin Shen, Michael Holinstat, Joshua D. Brooks,
Emmanuele DiBenedetto, and Heidi E. Hamm‡

From the Department of Pharmacology, Vanderbilt University Medical Center, Department of Mathematics and Center for Biomathematics, Vanderbilt University, Nashville, Tennessee 37232

Thrombin activates protease-activated receptor-1 (PAR-1) by cleavage of the amino terminus to unmask a tethered ligand. Although peptide analogs can activate PAR-1, we show that the functional responses mediated via PAR-1 differ between the agonists. Thrombin caused endothelial monolayer permeability and mobilized intracellular calcium with EC₅₀ values of 0.1 and 1.7 nM, respectively. The opposite order of activation was observed for agonist peptide (SFLLRN-CONH₂ or TFLLRNKPKDK) activation. The addition of inactivated thrombin did not affect agonist peptide signaling, suggesting that the differences in activation mechanisms are intramolecular in origin. Although activation of PAR-1 or PAR-2 by agonist peptides induced calcium mobilization, only PAR-1 activation affected barrier function. Induced barrier permeability is likely to be G $\alpha_{12/13}$ -mediated as chelation of G α_q -mediated intracellular calcium with BAPTA-AM, pertussis toxin inhibition of G $\alpha_{i/o}$, or GM6001 inhibition of matrix metalloproteinase had no effect, whereas Y-27632 inhibition of the G $\alpha_{12/13}$ -mediated Rho kinase abrogated the response. Similarly, calcium mobilization is G α_q -mediated and independent of G $\alpha_{i/o}$ and G $\alpha_{12/13}$ because pertussis toxin and Y-27632 had no effect, whereas U-73122 inhibition of phospholipase C- β blocked the response. It is therefore likely that changes in permeability reflect G $\alpha_{12/13}$ activation, and changes in calcium reflect G α_q activation, implying that the pharmacological differences between agonists are likely caused by the ability of the receptor to activate G $\alpha_{12/13}$ or G α_q . This functional selectivity was characterized quantitatively by a mathematical model describing each step leading to Rho activation and/or calcium mobilization. This model provides an estimate that peptide activation alters receptor/G protein binding to favor G α_q activation over G $\alpha_{12/13}$ by ~800-fold.

Classical receptor theory presents a model in which a single functional response is intrinsically associated with a given G protein-coupled receptor (GPCR).¹ However, there is growing

* This work was supported by National Institutes of Health Grant 5P01 HL60678 and 5R01 GM068953, Keck Futures Initiatives/NAKFI Sig05 (to H. E. H.). The costs of publication of this article were defrayed in part by the payment of page charges. This article must therefore be hereby marked "advertisement" in accordance with 18 U.S.C. Section 1734 solely to indicate this fact.

[§] The on-line version of this article (available at <http://www.jbc.org>) contains a supplemental figure.

‡ To whom correspondence should be addressed: Dept. of Pharmacology, Vanderbilt University Medical Center, 444 Robinson Research Bldg., 23rd Ave. South at Pierce, Nashville, TN 37232-6600. Tel.: 615-343-3533; Fax: 615-343-1084; E-mail: heidi.hamm@vanderbilt.edu.

¹ The abbreviations used are: GPCR, G protein-coupled receptor; AF,

evidence that diverse signaling responses can be invoked by single GPCRs in response to interaction with divergent ligands. This phenomenon of "agonist trafficking" or "ligand-induced functional selectivity" (or simply functional selectivity) stands in stark contrast to conventional receptor pharmacology.

Receptors such as the serotonin (1–3), β_2 -adrenergic (4), dopamine (5, 6), octopamine (7), and others continue to expand the diversity of receptor families which demonstrate functional selectivity (for a recent reviews, see Refs. 8 and 9). We show here that two different protease-activated receptor-1 (PAR-1) agonist peptides, SFLLRN-CONH₂ and the PAR-1-specific TFLLRNKPKDK, activate PAR-1 in a fashion different from that of thrombin-mediated cleavage of the amino terminus of the receptor. This was accomplished by investigating two functionally different endothelial responses: 1) induced endothelial barrier permeability and 2) induced intracellular calcium mobilization. When compared, the ability of thrombin or agonist peptide to elicit these responses was significantly different.

The vascular endothelium serves as a regulated barrier between the bloodstream and the interstitial tissues. Thrombin is a major inflammatory factor that mediates the contraction of endothelial cells leading to increased permeability of the barrier and vascular edema. Although antagonists have recently been developed to target PAR-1 (10) and PAR-4 (11), currently there is no way to inhibit the effects of thrombin on vascular edema selectively except by inhibiting thrombin, which also inhibits clotting and leads to increased risks of bleeding disorders. Inhibition of PAR signaling in the endothelium without disabling the role of thrombin in hemostasis would be more therapeutically beneficial.

The four isoforms of PAR-1 form a unique class of GPCRs. Activated by proteolytic cleavage of the extracellular amino terminus, the newly exposed terminus serves as a tethered ligand, folding back onto the receptor, thereby activating it. Unlike the other PARs, which are cleaved by the protease thrombin, PAR-2 is trypsin- and not thrombin-sensitive (12). In humans, PAR-1 and PAR-2 are thought to mediate signaling in the endothelium, whereas PAR-1 and PAR-4 are thought to mediate signaling in platelets (13). Interestingly, the signaling properties of PAR-3 are still unclear. To date there is no clear evidence that PAR-3 can participate in intracellular signaling

AYPGKF-CONH₂; ECIS, electric cell-substrate impedance sensor; GAP, GTPase-activating protein; GEF, guanine nucleotide exchange factor; GST-RBD, glutathione S-transferase-rhotekin-Rho-binding domain; HMEC-1, human microvascular endothelial cells; HUVEC, human umbilical vein endothelial cells; IP₃, inositol trisphosphate; MMP, matrix metalloproteinase; MLC, myosin light chain; PAR, protease-activated receptor; PBS, phosphate-buffered saline; PLC- β , phospholipase C- β ; PTX, pertussis toxin; SN, SFLLRN-CONH₂; SV, SLIGKV; TER, transendothelial electrical resistance; TK, TFLLRNKPKDK; YP, YFLLRNP.

(14–16), although its role as a cofactor in mouse platelet activation of PAR-4 has been determined (17).

Activated by thrombin, PAR-1 exerts its effects on the endothelium by concomitant activation of the $G_{\alpha_{i/o}}$, G_{α_q} , and $G_{\alpha_{12/13}}$ families of G proteins (18, 19). These signals ultimately integrate to induce profound changes in vascular endothelial cells, including increased endothelial monolayer permeability (20–22).

Activation of Rho plays a significant role in endothelial barrier function. The discovery of Rho-guanine nucleotide exchange factors (GEFs) as effectors of $G_{\alpha_{12/13}}$ (p115RhoGEF (23), LARG (24), PDZ RhoGEF (25) and GTRAP48 (26)) has completed one pathway between PAR-1 and Rho activation. However, it is also well established that in primary endothelial cells, thrombin-induced barrier permeability is dependent not only upon Rho activation but also calcium mobilization (27–31). To the contrary, we show here that in the transformed cell line human microvascular endothelial cells (HMEC-1), thrombin-induced barrier permeability is dependent solely upon a Rho kinase-mediated pathway initiated by $G_{\alpha_{12/13}}$ activation and not G_{α_q} or $G_{\alpha_{i/o}}$. We also show that thrombin-induced calcium mobilization is mediated by G_{α_q} and not by $G_{\alpha_{12/13}}$ or $G_{\alpha_{i/o}}$.

In addition to activation by proteolytic cleavage, PARs have been shown to be fully responsive to synthetic peptides that mimic the amino acid sequence of the tethered ligand portion of the receptor (32, 33). In addition to the direct tethered ligand sequence, SFLLRN, which has been shown to activate both PAR-1 and PAR-2 receptors, substitution of the Ser to Thr creates a new peptide with increased specificity for PAR-1 activation (34).

Although these agonist peptides appear to elicit full responses, there is an emerging body of evidence which suggests that agonist peptides do not activate PAR-1 in the same manner as does thrombin (35–39). In addition, activation of PAR-1 by other proteases has shown differential signaling (40). We show here that the rank order of potency for induced endothelial monolayer permeability and calcium mobilization differs between agonist peptide and thrombin activation of PAR-1.

To address the underlying mechanism, we have constructed a mathematical model containing 60 ordinary differential equations, which describes each known step leading to Rho activation as well as calcium mobilization. Our experimental observations in conjunction with our mathematical simulations have led us to hypothesize that the ability of PAR-1 to activate $G_{\alpha_{i/o}}$, G_{α_q} , or $G_{\alpha_{12/13}}$ is different with different agonists. Our data suggest that PAR-1 shows ligand-induced functional selectivity, with agonist peptides activating PAR-1 in such a way as to enhance G_{α_q} and/or decrease $G_{\alpha_{12/13}}$ signaling pathways compared with activation by thrombin.

EXPERIMENTAL PROCEDURES

Reagents—All cell culture reagents were purchased from Invitrogen. α -Thrombin (specific activity 3181 NIH units/mg protein), the thrombin inhibitor Z-D-Phe-Pro-methoxypropylboroglycinepinanediol ester, U-73122, GM6001, pertussis toxin, and Y-27632 were purchased from Calbiochem. The agonist peptides TFLLRNPKDK (TK), SFLLRN-CONH₂ (SN), SLIGKV (SV), AYPGKF-CONH₂ (AF), and YFLLRNP (YP) were purchased from GL Biochem (Shanghai) Ltd. BAPTA-AM and Alexa Fluor 568-phalloidin were purchased from Molecular Probes (Eugene, OR). Rho-A antibody anti-rabbit protein A/G was purchased from Santa Cruz (Santa Cruz, CA). Rho activation kits were purchased from Cytoskeleton, Inc. (Denver, CO).

Endothelial Cell Culture—In the present studies a human dermal microvascular endothelial cell line that was transformed using SV-40 was used (HMEC-1; obtained from Dr. E. Ades, Centers for Disease Control, Atlanta, GA). The cells were maintained in MCDB 131 medium supplemented with 5% fetal bovine serum, penicillin/streptomycin (5,000 units/ml; 5,000 μ g/ml), hydrocortisone (500 μ g/ml), epidermal growth factor (0.01 μ g/ml), and L-glutamine (2 mM) in an atmosphere of 95% air, 5% CO₂ at 37 °C. The cells were seeded at 1×10^5 cells/ml and

subcultured after detachment with 0.05% trypsin, 0.5 mM EDTA. All studies utilized cell passages 15–20.

Transendothelial Electrical Resistance (TER)—*In vitro* barrier permeability was monitored by electric cell-substrate impedance sensor (ECIS) (41). Gold electrodes were purchased from Applied BioPhysics (Troy, NY). Wells were coated in 0.1% gelatin prior to being wetted by culture media. After treatment, cells were seeded at 2×10^5 cells/well and allowed to recover for 24 h. The small and larger counter electrodes were connected to a phase-sensitive lock-in amplifier. A constant current of 1 μ A was applied by a 1-V, 4,000-Hz AC signal connected serially to a 1-megohm resistor between the small and large counter electrodes. The voltage between the small electrode and the large counter electrode was monitored by a lock-in amplifier, stored, and processed by a personal computer. The same computer controlled the output of the amplifier and switched the measurement to different electrodes in the course of the experiment. Prior to the experiments, the monolayers were serum starved for 18 h.

Calcium Mobilization—Cells were grown to confluence in black/clear bottom 96-well assay plates. Prior to the experiments, cells were serum starved for 18 h. All assays utilized the FLIPR Calcium Plus kit (Molecular Devices, Sunnyvale, CA). Cells were loaded with the calcium-sensitive dye and incubated for 1 h at 37 °C according to the manufacturer's protocols. The addition of agonists was robotically controlled, and samples were read by the FlexStation (Molecular Devices). Cells were excited at 485 nm and monitored at 515 nm.

BAPTA-AM Treatment—Cells were split, cultured, and serum starved as described according to the type of experiment being performed. Cells were then treated with 3 μ M BAPTA-AM and incubated at 37 °C for 3 h prior to stimulation.

[³²P]ADP-ribosylation—Complete ribosylation of $G_{\alpha_{i/o}}$ by pertussis toxin was determined as described previously (42–44). Briefly, cells were grown to confluence in 100-mm dishes and treated with 0.1 μ g/ml pertussis toxin (PTX) for 0.5, 1.0, 2.0, 3.0, or 18 h. Plasma membranes were isolated and subjected to a second round of ADP-ribosylation *in vitro* in the presence of nicotinamide adenine [³²P]NAD; Amersham Biosciences) to determine the amount of toxin substrate remaining. Membranes were harvested after two rinses with PBS in ice-cold TE buffer (25 mM Tris, pH 7.6, 0.1 mM EDTA, 1 mM phenylmethylsulfonyl fluoride, 10 μ g/ml pepstatin A, 10 μ g/ml leupeptin, and 1 μ g/ml aprotinin). Cell lysate was homogenized by titration seven times through a 25-gauge needle. Cellular debris was removed by low speed centrifugation (500 $\times g$ for 10 min). Supernatants were transferred to fresh tubes, and members were precipitated by centrifugation (40,000 $\times g$ for 60 min). Membranes were resuspended in 120 μ l of TE buffer and total protein determined using a BCA protein assay (Pierce) according to the manufacturer's protocols. PTX was activated by incubation in 25 mM dithiothreitol for 30 min at 37 °C. 40 μ g of purified membranes was incubated with 5 μ g/ml PTX in reaction buffer (2.5 μ M NAD, 1 mM ATP, 1 mM GTP, 10 mM thymidine, 6 mM MgCl₂, 2 mM EDTA, 2 mM dithiothreitol, 20 mM Tris, pH 7.6, and 25 μ Ci/ml [³²P]NAD) in a total volume of 200 μ l. Reactions were allowed to proceed at 37 °C for 60 min. Reactions were quenched by the addition of 20 μ l of ice-cold 100% (w/v) trichloroacetic acid. Membranes were precipitated by centrifugation (12,000 $\times g$ for 20 min) and resuspended in 15 μ l of 4 \times Laemmli loading buffer. Samples were boiled for 5 min, resolved by SDS-PAGE, and visualized by autoradiography.

Matrix Metalloproteinase (MMP) Inhibition—HMEC-1 were cultured to be used in calcium mobilization or induced monolayer permeability assays as described above. 30 min prior to stimulation with agonist, cells were treated with a final concentration of 25 μ M GM6001 to inhibit MMP-1, -2, -3, -8, and -9 or an equivalent volume of dimethyl sulfoxide as a vehicle control. Cells were then stimulated with subsaturating concentrations of either thrombin or TK, 2.0 nM or 1.0 μ M, respectively, for calcium mobilization or 0.2 nM thrombin or 2.0 μ M TK for induced permeability. Assays were then performed as described above. To ensure inhibition of MMPs by GM6001, HMEC-1 were split in to 6-well plates, allowed to recover for 48 h, and serum starved 24 h. Then they were pretreated with 25 μ M GM6001 or dimethyl sulfoxide as a control for 30 min and stimulated with 10 nM thrombin or serum-free medium as a base-line control. The culture medium was then harvested, and MMP activity was determined fluorescently using a gelatinase activity assay as described previously (45, 46).

Measurement of Rho Activity—Rho activity was measured using glutathione S-transferase-rhotekin-Rho-binding domain (GST-RBD) that specifically pulls down activated Rho (30, 47). HMEC-1 were serum-deprived for 1 h. Cells were then stimulated with various concentrations of thrombin for several time points, washed quickly with ice-cold Tris-buffered saline, and lysed in 500 μ l of lysis buffer (50 mM Tris, pH

TABLE I
Reactions used to describe thrombin and TK activation of intracellular calcium mobilization and Rho activation in HMEC-1
Concentration units are in molar and time in seconds in their respective contexts.

k_1 or K_m	k_{-1} or k_{cat}	Reaction	Reference
Reactions governing PAR-1 activation			
6.0E+04	1.0E-03	$AP + R \rightleftharpoons R^*$	(104)
2.0E-01		$AP \rightarrow \text{null}$	
1.3E-06	1.07E+02	$T + R \rightleftharpoons TR \rightarrow T + R^*$	(105)
1.5E-01		$T \rightarrow \text{null}$	(106)
2.0E+01		$R^* \rightarrow \text{null}$	
Reactions governing IP ₃ generation			
1.0E+08	1.0E+00	$R^* + G_q \cdot \text{GDP} \cdot \beta\gamma \rightleftharpoons R^* \cdot G_q \cdot \text{GDP} \cdot \beta\gamma$	(72)
5.0E+00	1.0E+06	$R^* \cdot G_q \cdot \text{GDP} \cdot \beta\gamma \rightleftharpoons R^* \cdot G_q \cdot \beta\gamma + \text{GDP}$	(72)
1.0E+06	1.0E-01	$R^* \cdot G_q \cdot \beta\gamma + \text{GTP} \rightleftharpoons R^* \cdot G_q \cdot \text{GTP} \cdot \beta\gamma$	(72)
2.0E+00	1.0E+07	$R^* \cdot G_q \cdot \text{GTP} \cdot \beta\gamma \rightleftharpoons R^* + G_q \cdot \text{GTP} + \beta\gamma$	(72)
2.0E-02		$G_q \cdot \text{GTP} \rightarrow G_q \cdot \text{GDP}$	(107-109)
5.0E+08	5.0E+00	$\text{PLC-}\beta + G_q \cdot \text{GTP} \rightleftharpoons \text{PLC-}\beta \cdot G_q \cdot \text{GTP}$	(109,110)
1.5E+01		$\text{PLC-}\beta \cdot G_q \cdot \text{GTP} \rightarrow \text{PLC-}\beta \cdot G_q \cdot \text{GDP}$	(108,109)
1.0E+05	1.0E+02	$\text{PLC-}\beta \cdot G_q \cdot \text{GDP} \rightleftharpoons \text{PLC-}\beta + G_q \cdot \text{GDP}$	(75)
1.0E+09	1.0E+00	$\text{PLC-}\beta \cdot G_q \cdot \text{GTP} + \text{PIP}_2 \rightleftharpoons \text{PLC-}\beta \cdot G_q \cdot \text{GTP} \cdot \text{PIP}_2^a$	(75)
1.0E+02		$\text{PLC-}\beta \cdot G_q \cdot \text{GTP} \cdot \text{PIP}_2^a \rightarrow \text{PLC-}\beta \cdot G_q \cdot \text{GTP} + \text{IP}_3$	(75)
2.4E-02		$\text{IP}_3 \rightarrow \text{null}$	
Reactions governing Ca ²⁺ mobilization			
			Reactions and constants for [Ca ²⁺] _i as described previously (74)
Reactions governing Rho activation			
1.0E+08	1.0E+00	$R^* + G_{13} \cdot \text{GDP} \cdot \beta\gamma \rightleftharpoons R^* \cdot G_{13} \cdot \text{GDP} \cdot \beta\gamma$	(72)
6.0E+00	1.0E+06	$R^* \cdot G_{13} \cdot \text{GDP} \cdot \beta\gamma \rightleftharpoons R^* \cdot G_{13} \cdot \beta\gamma + \text{GDP}$	(72)
1.0E+06	1.0E-01	$R^* \cdot G_{13} \cdot \beta\gamma + \text{GTP} \rightleftharpoons R^* \cdot G_{13} \cdot \text{GTP} \cdot \beta\gamma$	(72)
2.0E+00	1.0E+07	$R^* \cdot G_{13} \cdot \text{GTP} \cdot \beta\gamma \rightleftharpoons R^* + G_{13} \cdot \text{GTP} + \beta\gamma$	(72)
4.0E-03		$G_{13} \cdot \text{GTP} \rightarrow G_{13} \cdot \text{GDP}$	(23,111)
1.0E+09	3.0E+00	$\text{GEF} + G_{13} \cdot \text{GTP} \rightleftharpoons \text{GEF} \cdot G_{13} \cdot \text{GTP}$	(109)
1.0E-02		$\text{GEF} \cdot G_{13} \cdot \text{GTP} \rightarrow \text{GEF} \cdot G_{13} \cdot \text{GDP}$	(23)
1.0E+06	3.0E+00	$\text{GEF} \cdot G_{13} \cdot \text{GDP} \rightleftharpoons \text{GEF} + G_{13} \cdot \text{GDP}$	
7.7E+09	7.7E+02	$\text{GEF} \cdot G_{13} \cdot \text{GTP} + \text{RhoGDP} \rightleftharpoons \text{GEF} \cdot G_{13} \cdot \text{GTP} \cdot \text{RhoGDP}$	
1.03E+04		$\text{GEF} \cdot G_{13} \cdot \text{GTP} \cdot \text{RhoGDP} \rightarrow \text{GEF} \cdot G_{13} \cdot \text{GTP} + \text{RhoGTP}$	
6.0E-02		$\text{RhoGTP} \rightarrow \text{RhoGDP}$	(112)

^a PIP₂, phosphoinositide bisphosphate.

7.5, 10 mM MgCl₂, 0.5 M NaCl, 1% Triton X-100, 0.5% sodium deoxycholate, 0.1% SDS, 500 μg/ml tosyl arginine methyl ester, 10 μg/ml each leupeptin and aprotinin). Cell lysates were immediately centrifuged at 8,000 rpm at 4 °C for 5 min, and equal volumes of lysates were incubated with 30 μg of GST-RBD beads for 1 h at 4 °C. The beads were washed three times with wash buffer (25 mM Tris, pH 7.5, 30 mM MgCl₂, 40 mM NaCl), and bound Rho was eluted by boiling each sample in Laemmli sample buffer. Eluted samples from the beads and total cell lysate were then electrophoresed on 12.5% SDS-polyacrylamide gels, transferred to nitrocellulose, blocked with 5% nonfat milk, and analyzed by Western blotting using a polyclonal anti-Rho-A antibody.

Actin Stress Fibers—Cells were stimulated for 5 min with 10 nM α-thrombin, 10 μM SN, 10 μM TK, or 100 μM SV, rinsed quickly with ice-cold Hanks' balanced salt solution, and fixed with 4% paraformaldehyde. Cells were permeabilized for 3 min with 0.1% Triton X-100 in Hanks' balanced salt solution followed by incubation for 20 min with 1% bovine serum albumin. Cells were then incubated with Alexa Fluor 568-phalloidin to label stress fibers. After incubation, cells were rinsed six times with Hanks' balanced salt solution and mounted on slides using Prolong antifade mounting kit. Cells were viewed with a Zeiss LSM-510 confocal microscope using CY3 filter.

Mathematical Modeling—The biochemical pathways initiated by either agonist peptide or thrombin activation of PAR-1 resulting in Rho activation and/or intracellular calcium mobilization (see Fig. 5) were translated into a system of ordinary differential equations (Table I). These reactions were then solved using MatLab (The MathWorks Inc., Natick, MA) on a Linux-based operating system with the initial conditions listed in Table II.

TABLE II
Initial conditions and additional constants used in simulations

Species	Concentration	Reference
<i>M</i>		
R	6.0E-09	(113)
G _q GDP·βγ	4.3E-09	
GTP	1.0E-06	
PLC-β	3.0E-09	
PIP ₂ ^a	2.0E-06	
IP ₃ R	1.0E-09	
Ca ²⁺	5.5E-08	
G ₁₃ GDP·βγ	4.3E-09	
GEF	3.0E-09	
RhoGDP	3.0E-09	

^a PIP₂, phosphoinositide bisphosphate.

RESULTS

Differences between Thrombin and Agonist Peptide Activation—The effects of agonist peptides were compared with those of thrombin stimulation using two functionally different assays of PAR-1 activation: 1) induced endothelial barrier permeability and 2) induced intracellular calcium mobilization. The following agonist peptides were utilized in these studies: the exact PAR-1 tethered ligand SFLLRN-CONH₂ (SN), which activates both PAR-1 and PAR-2; the PAR-1-specific agonist peptide TFLLRNKPKDK (TK); the PAR-2-specific agonist pep-

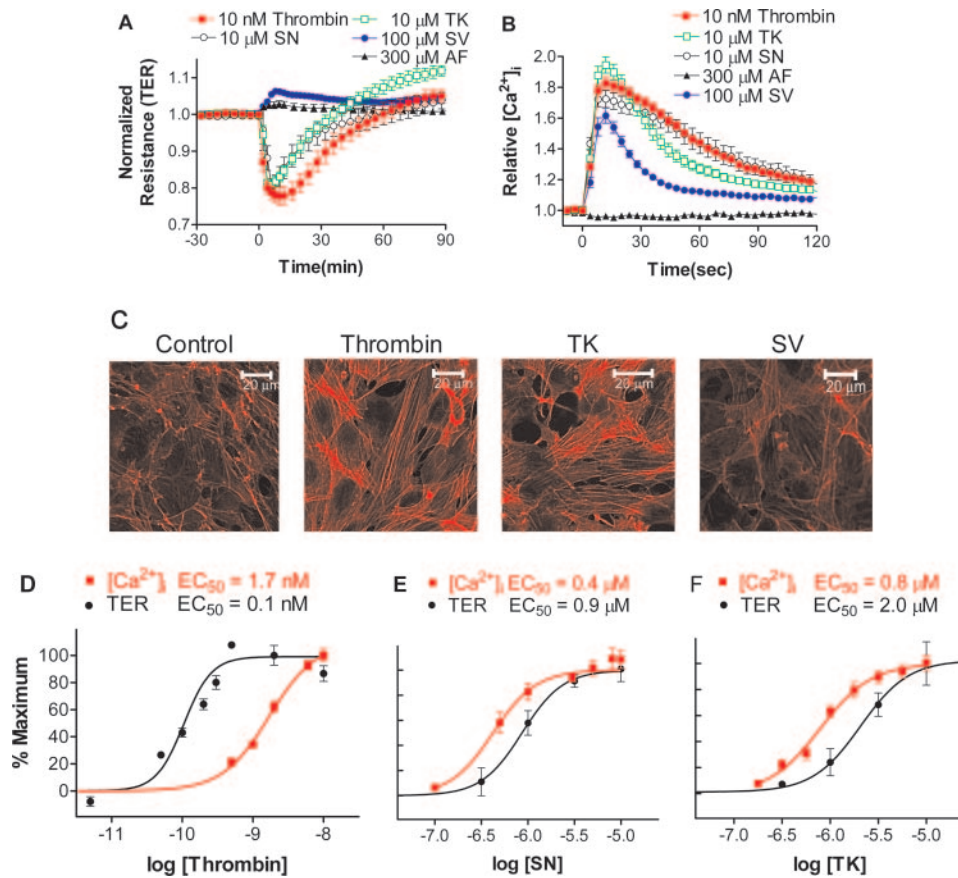


FIG. 1. Differences between thrombin and agonist peptide activation of PAR-1 and PAR-2. Changes in TER and intracellular calcium mobilization were determined in HMEC-1 stimulated with thrombin, a PAR-1 and PAR-2 activating peptide SN, the PAR-1-specific agonist peptide TK, the PAR-2-specific agonist peptide SV, or the PAR-4-specific agonist peptide AF. Changes in barrier function were monitored using ECIS (A) and $[Ca^{2+}]_i$ mobilization were determined using the FlexStation (B). Filled red squares, 10 nM thrombin; open black circles, 10 μM SN; open green squares, 10 μM TK; filled blue circles, 100 μM SV; filled black triangles, 300 μM AF. C, actin stress fiber formation was determined by rhodamine-phalloidin staining and visualized using confocal microscopy after stimulation with PBS (control), 10 nM thrombin, 10 μM TK, or 100 μM SV for 5 min. Panels are representative images of at least two independent experiments. D, cells were treated under the same experimental conditions as in A stimulated with 0.001–10.0 nM thrombin. The minimum in TER at each concentration of thrombin was determined and normalized to the maximum response and plotted as a function of thrombin concentration (black circles). Cells were also treated under the same experimental conditions as in B, stimulated with 0.001–10.0 nM thrombin. The maximum -fold increase in calcium mobilization at each concentration of thrombin was determined and normalized to the maximum response and plotted as a function of thrombin concentration (red squares). E, cells were treated and assayed as in D except they were stimulated with 0.316–10.0 μM SN for TER (black circles) or 0.1–100.0 μM SN for calcium mobilization (red squares). F, cells were treated and assayed as in D except they were stimulated with 0.316–100.0 μM TK for TER (black circles) or 0.18–10.0 μM TK for calcium mobilization (red squares). Each point represents the average of between three and nine independent experiments. Error bars represent the S.E.

tide SLIGKV (SV) (48, 49); and the PAR-4-specific agonist peptide AYPGKF-CONH₂ (AF) (50).

PAR-1-induced endothelial barrier permeability was monitored by ECIS. HMEC-1 were grown on gold electrodes, and the TER was measured in response to agonist. Fig. 1A shows the changes in TER in response to saturating amounts of thrombin (10 nM), SN (10 μM), TK (10 μM), SV (100 μM), or AF (300 μM). Only those agonists that can activate PAR-1, *i.e.* thrombin, SN, and TK, induced barrier permeability to approximately the same extent (25–30%) and fully recovered by 90 min. Neither the PAR-2-specific nor the PAR-4-specific agonist peptide had any effect. Even though the absolute resistances before stimulation in all experiments were comparable, TK appeared to rebound, creating a tighter barrier. These data indicate both thrombin and PAR-1 but not PAR-2 agonist peptides induce barrier permeability.

To determine whether thrombin and agonist peptides mobilize intracellular calcium ($[Ca^{2+}]_i$) differently, calcium transients were measured real time using the FlexStation. Fig. 1B is a comparison of the resulting traces. Saturating amounts of each agonist induced a ~2-fold increase in $[Ca^{2+}]_i$. The data indicate that thrombin and both PAR-1 and PAR-2 agonist

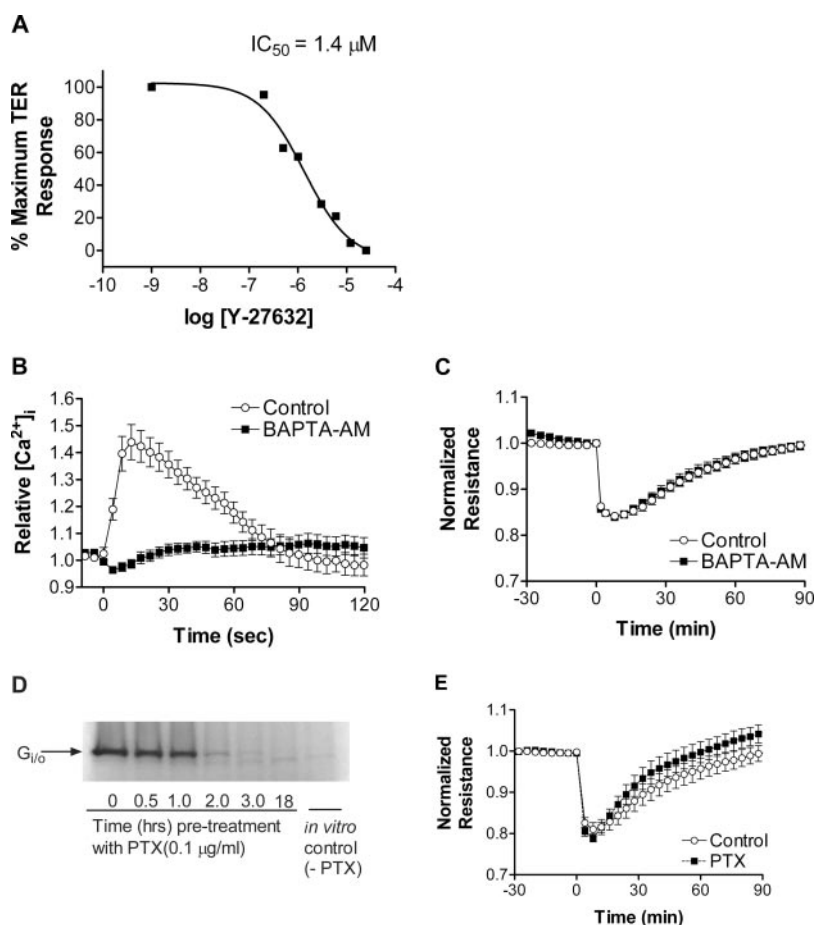
peptides induce similar $[Ca^{2+}]_i$ mobilization. The PAR-4-specific agonist peptide failed to elicit a calcium response. The viability of the PAR-4 agonist peptide was confirmed in platelets which have been shown to express the receptor, mobilizing $[Ca^{2+}]_i$ comparable with thrombin at < 300 μM AF (data not shown).

Endothelial cells have been shown to express PAR-1, -2, and -3 but not PAR-4 (51). The lack of response to the PAR-4-specific agonist peptide in both the TER and calcium assays implies that PAR-4 is not expressed in HMEC-1. This supposition was confirmed via reverse transcription-PCR (data not shown). As in other endothelial cells, thrombin signaling is therefore most likely to occur via PAR-1 and not PAR-4.

The PAR-1 partial agonist peptide YFLLRNP (YP) has been shown to activate platelet shape change without mobilizing calcium stores (52–58). In HMEC-1 we found YP to have no effect on induced barrier permeability (data not shown).

Because SV was the only agonist that induced calcium mobilization but not barrier permeability, it was important to characterize further its effects on the signaling cascade upstream of barrier function. Actin stress fiber formation is required for and precedes induced barrier permeability (59). Re-

FIG. 2. Thrombin-induced barrier permeability is Rho kinase-dependent and calcium- and $G\alpha_{i/o}$ -independent in HMEC-1. Changes in barrier function were monitored using ECIS, and $[Ca^{2+}]_i$ mobilization was determined using the FlexStation as in Fig. 1. *A*, cells were treated with increasing concentrations of the Rho kinase inhibitor Y-27632 (0.2–25.0 μM) 3 h prior to treatment with 0.5 nM thrombin. The minimum in TER at each concentration of Y-27632 was determined and normalized to the maximum response (■), and the IC_{50} was determined: 1.4 μM . *B*, cells were treated 3.0 μM BAPTA-AM (■) or 0.02% dimethyl sulfoxide (○) 1 h prior to stimulation with 10 nM thrombin. Intracellular calcium mobilization was assayed as before. *C*, cells were grown to confluence in gold electrodes and treated with 3.0 μM BAPTA-AM (■) or PBS as control (○) 1 h prior to stimulation with 10 nM thrombin. Changes in TER were determined by ECIS. *D*, cells were treated with 0.1 $\mu g/ml$ PTX. Membranes were harvested at the indicated times after treatment. Harvested membranes were subjected to a second round of PTX treatment in the presence of radiolabeled NAD as substrate. Samples were resolved by SDS-PAGE and visualized by autoradiography. *E*, cells were grown to confluence in gold electrodes and treated with 0.1 $\mu g/ml$ PTX for 18 h (■) or PBS as control (○) prior to stimulation with 10 nM thrombin. Changes in TER were determined by ECIS. Each panel is representative or depicts the average of at least three independent experiments. Error bars represent the S.E.



ceptors that couple to $G\alpha_q$ have been shown to induce stress fiber formation via activation of $G\alpha_{12/13}$ (60). Therefore, to determine whether activation of PAR-2 by SV might still stimulate $G\alpha_{12/13}$ resulting in stress fiber formation but fail to permeabilize the barrier, HMEC-1 were treated with vehicle, thrombin, TK, or SV, and actin stress fiber formation was determined by immunostaining and visualized by confocal microscopy (Fig. 1C). Both thrombin and TK readily induced stress fiber formation compared with control, whereas SV failed to induce a response. These data indicate that the effects of thrombin on induced barrier permeability are independent of PAR-2 signaling.

Dose-response curves were generated for each PAR-1 agonist, thrombin, SN, and TK, in calcium mobilization and induced monolayer permeability assays. Thrombin induced permeability with an EC_{50} of 0.1 (0.06–0.20) nM and mobilized calcium with an EC_{50} 1.7 (1.2–2.4) nM (Fig. 1D). The EC_{50} values were compared using the unpaired *t* test, and the *p* value was < 0.0001 , indicating that the values are statistically different. When stimulated with SN, the opposite rank order of activation was observed (Fig. 1E). SN mobilized calcium with an EC_{50} of 0.4 (0.3–0.6) μM and induced permeability with a higher EC_{50} of 0.9 (0.8–1.0) μM ; *p* value < 0.0038 .

To confirm that this was not an effect of nonspecific interactions between SN and PAR-2 affecting calcium mobilization, the experiments were repeated using the PAR-1-specific agonist peptide TK. TK mobilized calcium with an EC_{50} of 0.8 (0.6–1.0) μM and induced permeability with a higher EC_{50} 2.0 (1.6–2.6) μM ; *p* value of < 0.0013 . The dose-response curves for SN and TK were similar to each other, but opposite in order from those generated by thrombin. These data demonstrate that the agonist peptides do not activate PAR-1 in the same

fashion as thrombin. Because TK recapitulated, qualitatively, the reversal of relative EC_{50} values observed for SN stimulation compared with that of thrombin, to ensure PAR-1 specificity, TK was utilized in the remaining experiments.

$G\alpha_{12/13}$ Activation—To determine which G proteins, $G\alpha_{12/13}$, $G\alpha_q$, and/or $G\alpha_{i/o}$, activated by PAR-1 stimulation were responsible for changes in barrier function, either the G proteins themselves or individual downstream effectors were systematically inhibited. Rho is known to be activated by $G\alpha_{12/13}$ (23, 61) and induce barrier permeability via activation of Rho kinase (59). When Rho kinase was inhibited by pretreatment with Y-27632, the thrombin-induced decrease in TER was completely abrogated with an IC_{50} of 1.4 μM (Fig. 2A). These data indicate that Rho activation is necessary for and correlates directly with thrombin-induced barrier permeability.

To determine whether $G\alpha_q$ -mediated calcium release was necessary in PAR-1-induced barrier permeability, intracellular calcium was chelated by pretreatment with BAPTA-AM, and the effects on induced barrier permeability were determined. At 10 nM thrombin, 3 μM BAPTA-AM was sufficient to quench the intracellular calcium (Fig. 2B). However, BAPTA-AM had no effect on induced barrier permeability (Fig. 2C). This result suggests that Rho-dependent thrombin-induced barrier permeability in this system is calcium-independent.

PAR-2 is thought to couple with $G\alpha_{i/o}$ and $G\alpha_q$, but there is no evidence that it couples with $G\alpha_{12/13}$ (62). In addition, data from Fig. 1, A and B, demonstrate calcium originating from activation of PAR-2 does not induce barrier permeability in HMEC-1. The data confirm our observations that $[Ca^{2+}]_i$ mobilization is not requisite to induce barrier permeability in HMEC-1 (Fig. 2C).

To address the possibility that $G\alpha_{i/o}$ activation and/or release

of $G\beta\gamma$ affects barrier function, HMEC-1 were pretreated with PTX to inhibit $G\alpha_{i/o}$ subunits by ADP-ribosylation. PTX treatment was controlled for by a substrate depletion assay. Pretreatment with PTX for 18 h completely inactivated all $G\alpha_{i/o}$ subunits (Fig. 2D). However, PTX treatment had no effect on TER (Fig. 2E), suggesting that $G\alpha_{i/o}$ has no effect on induced permeability. This result differs from that which has been published previously (19). This difference might be attributed to different lots and passage numbers for the cells used or differences in experimental conditions.

When taken together, these results would suggest that $G\alpha_{i/o}$ and/or the $G\beta\gamma$ subunits liberated by their activation as well as $G\alpha_q$ -mediated intracellular calcium fluxes do not affect and therefore do not integrate in a significant way with the Rho-dependent signaling network, which controls thrombin-induced barrier permeability in HMEC-1. This conclusion would imply that PAR-1-mediated monolayer permeability can be used as a measure for $G\alpha_{12/13}$ activation.

$G\alpha_q$ Activation—Thrombin-induced $[Ca^{2+}]_i$ mobilization is thought to occur via PAR-1 activation of $G\alpha_q$ and subsequent stimulation of phospholipase C- β (PLC- β). In addition, $G\beta\gamma$ liberated from activation of $G\alpha_{i/o}$ has a high affinity for certain PLC- β isoforms, which interaction results in calcium mobilization (63). To verify that thrombin-induced calcium mobilization was occurring via a PLC- β -dependent pathway, HMEC-1 were pretreated with an inhibitor of PLC- β activation, U-73122 (64). Pretreatment with U-73122 for 30 min completely inhibited the calcium transients with an IC_{50} of $\sim 0.5 \mu M$ (Fig. 3A). These data indicate that activation of PLC- β by PAR-1 is requisite for calcium mobilization.

To determine whether PLC- β activation was occurring via $G\beta\gamma$ subunits liberated from activation of $G\alpha_{i/o}$, HMEC-1 were pretreated with or without PTX as before. There were no differences in the dose-response curves between PTX-treated cells and control (Fig. 3B). Therefore, these results suggest $G\alpha_{i/o}$ does not significantly affect thrombin-induced calcium mobilization in HMEC-1.

Rho has been implicated in modulating calcium signaling in endothelial cells (65). To determine whether $G\alpha_q$ -mediated calcium mobilization was Rho kinase-dependent, HMEC-1 were treated with Y-27632. There was no difference between Y-27632 treatment and control cells (Fig. 3C). These data indicate that activation of $G\alpha_{12/13}$ and its subsequent effectors likely have no effect on calcium mobilization.

Taken together the results suggest that in HMEC-1 thrombin-induced changes in barrier permeability are dependent upon $G\alpha_{12/13}$ activation and function independently of either $G\alpha_q$ - or $G\alpha_{i/o}$ -mediated signaling cascades. Likewise, thrombin-induced calcium mobilization is mediated by $G\alpha_q$ activation and independent of $G\alpha_{12/13}$ and $G\alpha_{i/o}$. Therefore, it is reasonable to suggest that changes in permeability directly reflect $G\alpha_{12/13}$ activation, and changes in intracellular calcium directly reflect $G\alpha_q$ activation. Hence, the differences observed between thrombin and agonist peptide activation of PAR-1 could be explained by differences in the ability of the receptor to activate $G\alpha_{12/13}$ or $G\alpha_q$. This hypothesis would imply that agonist peptides induce the receptor to couple differently to its G protein families, suggesting that activation of PAR-1 by different agonists induces functional selectivity.

Effects of Catalytically Inactive Thrombin—Thrombin has been observed to induce differential cellular responses via proteolytic versus nonproteolytic pathways (66–69). To address whether the observed differences between thrombin and agonist peptide activation originate from nonproteolytic interactions of thrombin with PAR-1 or other thrombin receptors via protein-protein interactions outside of the catalytic pocket, 2

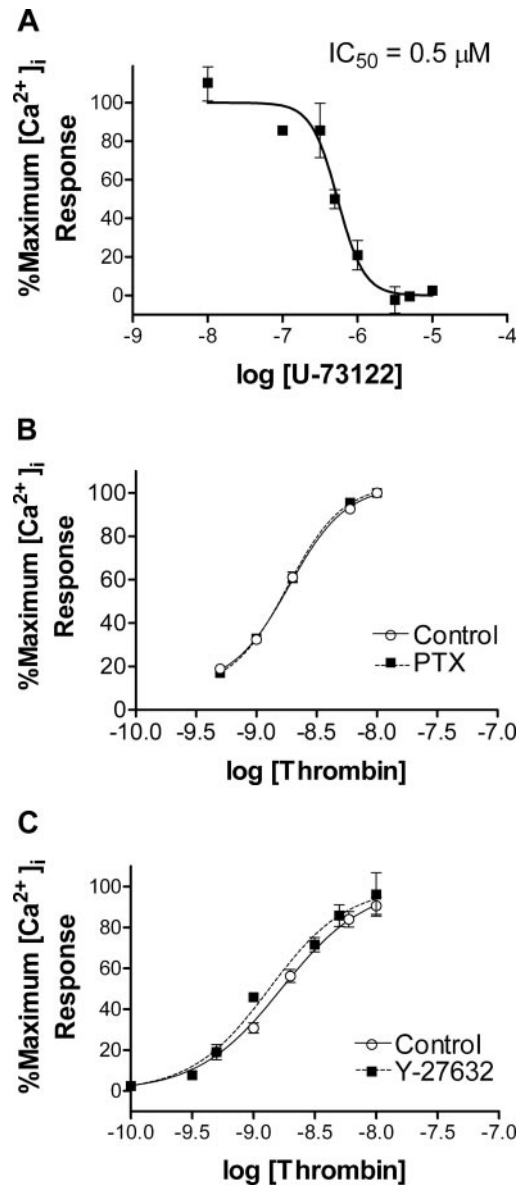


FIG. 3. Thrombin-induced intracellular calcium mobilization is PLC- β -dependent and $G\alpha_{i/o}$ - and Rho kinase-independent in HMEC-1. Intracellular calcium mobilization was determined using the FlexStation as in Fig. 1. *A*, cells were pretreated for 30 min with increasing concentrations of the PLC- β inhibitor U-73122 (0.01–10.0 μM) 30 min prior to treatment with 6.0 nM thrombin. The maximum -fold increase in calcium mobilization at each concentration of U-73122 was determined and normalized to the maximum response, and the IC_{50} was determined: 0.5 μM . *B*, cells were treated with 0.1 $\mu g/ml$ PTX (■) or PBS as control (○) 18 h prior to stimulation with increasing concentrations of thrombin (0.5–10.0 nM). $[Ca^{2+}]_i$ mobilization was assayed as before. The maximum -fold increase in calcium mobilization at each concentration of thrombin was determined and normalized to the maximum response. *C*, cells were treated with 1.2 μM Y-27632 (■) or PBS as control (○) 3 h prior to stimulation with increasing concentrations of thrombin (0.01–10.0 nM). $[Ca^{2+}]_i$ mobilization was assayed as before. The maximum -fold increase in calcium mobilization at each concentration of thrombin was determined and normalized to the maximum response. Each panel is representative or depicts the average of at least three independent experiments. Error bars represent the S.E.

nM thrombin was treated with or without the thrombin inhibitor Z-D-Phe-Pro-methoxypropylboroglycinepinanediol ester (0.2 or 1.0 μM), and calcium mobilization and induced monolayer permeability were then assayed as before. The thrombin inhibitor blocked thrombin-induced calcium mobilization and induced permeability, indicating that the inhibitor functioned as expected (Fig. 4A). When cells were stimulated with sub-

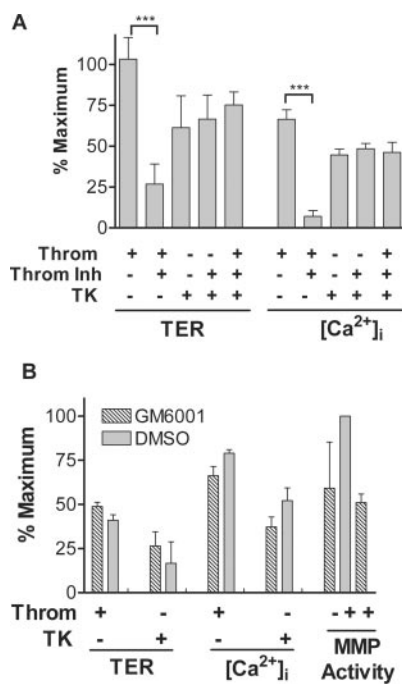


FIG. 4. Effects of nonenzymatic interactions of thrombin and inhibition of MMPs on PAR signaling. *A*, the effects of catalytically inactivated thrombin on agonist peptide-induced signaling were determined by assaying calcium mobilization and barrier permeability. HMEC-1 were treated with subsaturating concentrations of TK, 2 μM or 3 μM for calcium mobilization ($[\text{Ca}^{2+}]_i$) or permeability (TER), respectively, with, without, or only 2 nM thrombin that had been inactivated by a 10-min pretreatment with 0.2 or 1.0 μM thrombin inhibitor. Data represent at least three separate experiments. Statistical analysis was performed using the two-tailed *t* test. *** indicates *p* value < 0.001. *B*, HMEC-1 were pretreated with 25 μM GM6001, and the effects of MMP inhibition on monolayer permeability (TER) and intracellular calcium mobilization ($[\text{Ca}^{2+}]_i$) by stimulation with subsaturating concentrations of either thrombin (0.2 or 2.0 nM, in each assay, respectively) or agonist peptide (TK) (2.0 or 1.0 μM , respectively) were determined as before. Data represent at least three separate experiments. The effects of 25 μM GM6001 treatment on MMP activity was measured using a fluorescent gelatinase activity assay performed on harvested culture medium as described under "Experimental Procedures." Data represent at least two separate experiments. All samples were normalized to the maximum achievable response for each corresponding agonist in each assay. All results are shown as the mean \pm S.E. DMSO, dimethyl sulfoxide.

saturating concentrations of TK, the addition of 2 nM catalytically inactive thrombin had no effect in either assay. The concentrations of agonist used were chosen to be close to the EC_{50} for either induced barrier permeability or intracellular calcium mobilization. Hence, it is reasonable to conclude that a lack of effect at this dose would be reflected in a lack of change in the EC_{50} of the dose response. These results suggest that the effects of thrombin in each assay are the result of the catalytic function of thrombin and not a protein/protein interaction with PARs or other thrombin receptors or associated proteins present on the cell surface after cleavage of the receptor.

Inhibition of MMPs—MMPs play critical roles in controlling the structure of the extracellular matrix. Endothelial barrier function is closely connected with the extracellular matrix. For example, MMP-9 activity has been shown to induce monolayer permeability in bovine retinal endothelial cells (70). Several MMPs, including MMP-2 and -9, are secreted as inactive proenzymes by endothelial cells. However, thrombin has been shown to activate MMP-2 in endothelial cells (71). It was therefore necessary to determine whether activation of MMPs by proteolytic cleavage by thrombin was affecting thrombin-induced barrier permeability but not agonist peptide-mediated activation, hence causing the relative change in EC_{50} values observed in

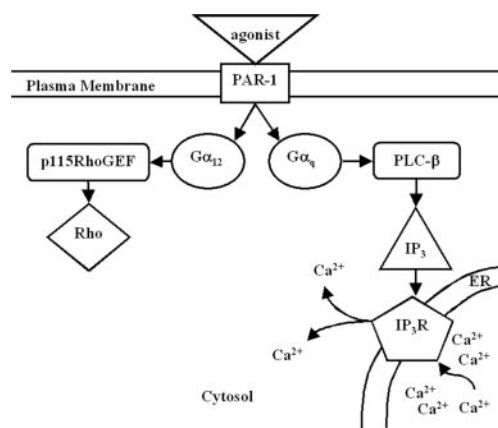


FIG. 5. Representation of the signaling pathways initiated by PAR-1 used to create a mathematical model. Both $\text{G}\alpha_{12/13}$ and $\text{G}\alpha_q$ -mediated pathways are initiated by PAR-1 activation. In HMEC-1 cultures, calcium mobilization is dependent upon $\text{G}\alpha_q$ and not $\text{G}\alpha_{12/13}$, whereas Rho activation is dependent upon $\text{G}\alpha_{12/13}$ and not $\text{G}\alpha_q$. To understand better the signaling properties of PAR-1, each enzymatic reaction or protein/protein interaction depicted here was translated into a system of differential reactions to generate a mathematical model describing the signaling event initiated by PAR-1 activation. The model was then used to predict differences experimentally observed between thrombin and agonist peptide forms of receptor activation.

Fig. 1. To accomplish this, HMEC-1 were pretreated with GM6001, a general MMP inhibitor that inhibits MMP-1, -2, -3, -8, and -9. Cells were then stimulated with subsaturating concentrations of either thrombin or TK and induced monolayer permeability or intracellular calcium mobilization was assayed as before. Fig. 4*B* shows that treatment with GM6001 inhibited MMP activity but had no effect in either assay compared with the vehicle control. The effect of GM6001 on MMP activity was determined using a fluorescent gelatinase activity assay. Thrombin treatment significantly increased the basal MMP activity. However, treatment with 25 μM GM6001 abolished the thrombin-induced MMP activity, bringing total MMP activity back down to basal.

Mathematical Modeling—To obtain a more global understanding of the quantitative relationships between these pathways and barrier function, a mathematical model was created which incorporated all biochemical reactions of these two pathways in HMEC-1. Fig. 5 is a scheme representing the proteins and interactions that were mathematically modeled. To construct the initial model, protein/protein interactions and enzymatic activations were translated into a system of ordinary differential reactions resembling well established models for receptor-G protein activation and calcium mobilization (72–75). Activation of the IP_3 receptor of the endoplasmic reticulum by IP_3 and calcium was modeled according to equations proposed by De Young and Keizer (74). Many of the known and experimentally determined kinetic parameters describing the system were extracted from the literature. Because the initial conditions, concentrations, and kinetic parameters for all components of the pathway have not been reported, we judiciously fixed those values (see Tables I and II). Model parameters were chosen to best fit the thrombin-induced calcium data experimentally determined here. Table I lists all of the parameters used in the model along with corresponding literature citations if applicable. Table II lists the initial conditions.

Initially, the model fit the calcium traces and thrombin dose-response curves already obtained. Fig. 6*A* shows a representative comparison between empirical data and simulations for calcium mobilization in response to 10 nM thrombin. At all concentrations of thrombin, experimental peak height fit with the simulations.

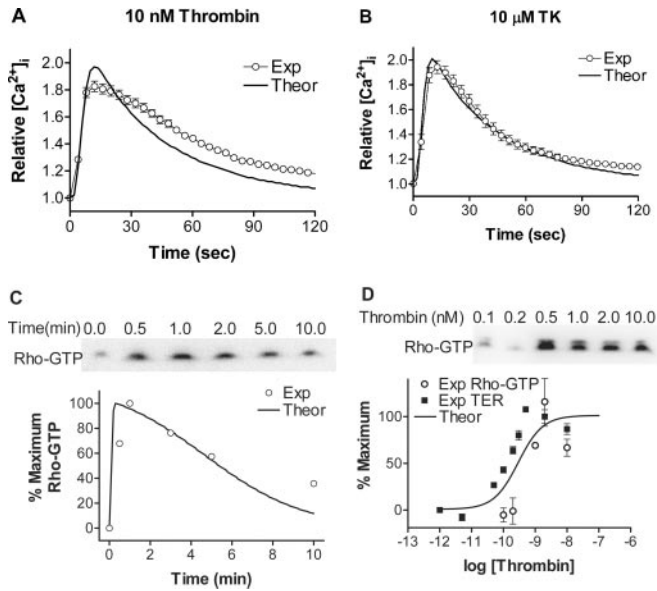


FIG. 6. Comparison between experimental results and theoretical simulations. Intracellular calcium mobilization was determined using the FlexStation. Experimental data (\circ) were compared with theoretical simulations (—) for 10 nM thrombin (A) or 10 μ M TK (B) stimulation. C, cells were cultured as before and stimulated with 10 nM thrombin. Signaling was quenched by cell lysis at the indicated times after stimulation. Activated Rho was determined by pull-down and visualized by immunoblot using an anti-Rho antibody. Equal loading was confirmed by immunoblot analysis of whole cell extract for total Rho. Experimental data for Rho activation (\circ) were compared with theoretical simulations (—). D, cells were cultured as before and stimulated with increasing concentrations of thrombin (0.1–10.0 nM). Signaling was quenched by cell lysis 1 min after stimulation. Activated Rho was determined as before. Experimental data for thrombin-induced barrier function (\blacksquare), Rho activation (\circ), and theoretical simulations of Rho activation (—) were compared. Barrier function and Rho activation correlate highly, differing in EC_{50} by < 3 -fold. Each panel is representative or depicts the average of at least three independent experiments. Error bars represent the S.E.

Calcium mobilization curves were fit to those experimentally obtained for TK. However, for this round of minimization, all parameters were kept constant except the binding kinetics for PAR-1 agonist peptide to the receptor. The simulations correlated well with the experimental data for TK-induced calcium mobilization (Fig. 6B).

To determine whether Rho activation could be correlated with, and therefore be used to model induced barrier permeability, Rho activation was assayed directly as a time course (Fig. 6C). These empirical data were well fit by the predicted curve of the mathematical model.

Similar experiments were carried out by stimulating HMEC-1 with increasing amounts of thrombin, quenching reactions at the point of maximal activation (Fig. 6D). The EC_{50} for thrombin-induced TER, Rho activation, and the theoretical prediction correlated and were not statistically different. These data, therefore, justify the use of mathematically representing Rho activation as a model for barrier permeability.

When the relative concentrations of G_{α_q} and $G_{\alpha_{12/13}}$ and the receptor-catalyzed activation efficiencies were mathematically set to be identical for each G protein, simulations predicted the EC_{50} for Rho activation to be ~ 10 -fold lower than that of calcium mobilization, that observed experimentally (Fig. 7A). However, the reversal observed for agonist peptide activation was not predicted by the initial model (Fig. 7B).

Simulations were run searching a variety of parameters that govern receptor activation and/or G protein activation such as the kinetics of GDP release from the heterotrimer which is thought to be rate-limiting in G protein activation (see supple-

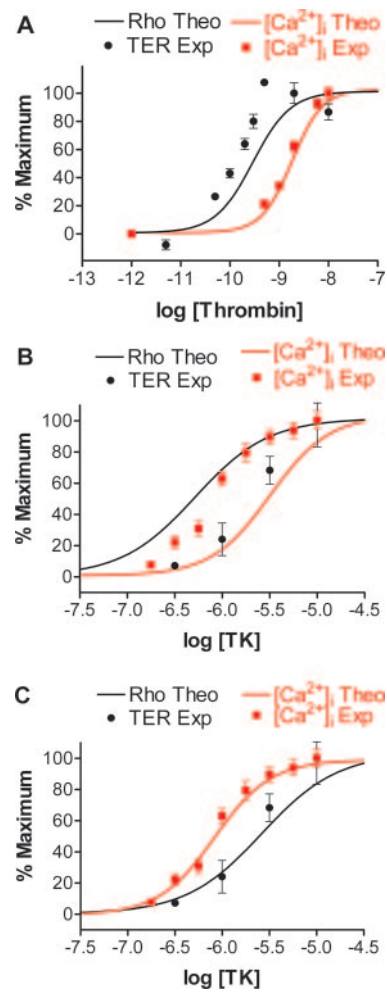


FIG. 7. Mathematical model predicts that PAR-1 activation by agonist peptide increases the affinity of the receptor to favor G_{α_q} over $G_{\alpha_{12/13}}$ by ~ 800 -fold. Initially, the theoretical concentrations and kinetics of receptor-mediated activation for both G_{α_q} and $G_{\alpha_{12/13}}$ were set to be identical. A, under these constraints, the model predicted the ~ 10 -fold difference in EC_{50} of induced barrier permeability and calcium mobilization observed in Fig. 1C (compare symbols (experimental data) with lines (simulations)). B, however, the model did not predict the reversal observed in Fig. 1D. Multiple parameters of the model were then manipulated in attempts to determine which states could predict the reversal (see supplemental figure). C, when the relative binding affinities of G_{α_q} or $G_{\alpha_{12/13}}$ for activated PAR-1 were changed from being equal ($G_{\alpha_q} + R^* \rightleftharpoons G_{\alpha_q}R^*$; $k_1 = 1E8$) and constrained to favor G_{α_q} (G_{α_q} : $k_1 = 2.5E9$; and $G_{\alpha_{12/13}}$: $k_1 = 3E6$) binding by ~ 800 -fold, the model predicted the observations for TK activation.

mental figure). One possible set of conditions was found which could predict the experimental observations: the ratio of the K_d for the activated receptor- G_{α_q} complex to the K_d for activated receptor- $G_{\alpha_{12/13}}$. When they were set to differ by ~ 800 -fold in favor of G_{α_q} activation, the curves switch activation order and match experiment data well (Fig. 7C).

DISCUSSION

Here we have explored the functional selectivity properties of PAR-1 by comparing the effects of agonist peptides or thrombin in induced endothelial barrier permeability and intracellular calcium mobilization in the endothelial cell line HMEC-1. At sufficiently high concentrations of the agonists, there appears to be no difference between thrombin and agonist peptide activation in either assay. However, we discovered that significant differences are masked by use of saturating concentrations of agonist. When dose-response curves were generated for thrombin or agonist peptides in each assay, differences in be-

tween their ability to activate G_{α_q} and $G_{\alpha_{12/13}}$ became apparent. Thrombin induces barrier permeability with an EC_{50} of ~ 0.1 nM and mobilizes calcium with a ~ 17 -fold greater EC_{50} . Importantly, when PAR-1 agonist peptides are used, the opposite rank order of activation is observed (compare Fig. 1D with 1, E and F).

Interestingly, we found that both PAR-1 and PAR-2 could mobilize calcium when activated by their selective agonist peptides to similar extents and with similar kinetics (Fig. 1B). Notably, however, unlike PAR-1, activation of PAR-2 had no effect on monolayer permeability (Fig. 1A), nor could it induce actin stress fiber formation (Fig. 1C). These data reveal that although PAR-1 and PAR-2 show significant sequence homology, having a 35% identity between human PAR-2 and human PAR-1 (76), their signaling properties are quite distinct. Similar differences have been observed by others in HUVEC (77). We have recapitulated those findings in a microvascular cell line, demonstrating that PAR-1-mediated permeability is dependent upon Rho activation. Taken together, these results suggest that a paramount difference between PAR-1 and PAR-2 activation is in their ability or inability to activate Rho GTPase.

In other endothelial cells, induced barrier permeability is dependent not only upon $G_{\alpha_{12/13}}$ -mediated Rho kinase activity (Fig. 2A), but also on calcium mobilization (27–31). Interestingly, in HMEC-1, when $[Ca^{2+}]_i$ was chelated with BAPTA-AM, there was no effect on thrombin-induced barrier permeability (Fig. 2, B and C). Nor did inhibition of $G_{\alpha_{i/o}}$ by PTX have any effect on PAR-1-induced barrier permeability (Fig. 2, D and E). In addition, calcium fluxes originating from PAR-2, which are similar to those induced by PAR-1, had no effect on the barrier. Taken together we interpret these results as meaning that induced barrier permeability in HMEC-1 by either thrombin or agonist peptides is dependent upon $G_{\alpha_{12/13}}$ activation by PAR-1 and is independent of G_{α_q} and $G_{\alpha_{i/o}}$, therefore it reflects $G_{\alpha_{12/13}}$ activation.

This difference in calcium dependence between endothelial cell types might be explained by differences in the mechanisms that result in myosin light chain (MLC) phosphorylation, which is thought to gate the final commitment step in induced endothelial cell contraction. Although MLC kinase can be regulated by $[Ca^{2+}]_i$ (78, 79), the MLC phosphatases are regulated by Rho kinase (80). Hence, activation of Rho in HMEC-1 could result in the inactivation of MLC phosphatases, favoring the phosphorylated state of MLC (30, 81, 82), making the pathway calcium-independent.

G_{α_q} -mediated calcium mobilization was found to be $G_{\alpha_{12/13}}$ - and $G_{\alpha_{i/o}}$ -independent. PLC- β , $G_{\alpha_{i/o}}$ and Rho kinase inhibition studies indicate that induced calcium mobilization occurs via G_{α_q} activation of PLC- β and is independent of $G_{\alpha_{12/13}}$ signaling (Fig. 3). We interpret these data as indicating that calcium mobilization is a representation of G_{α_q} activation. Although others have shown functional selectivity in other systems by observing either a reversal in rank order potency as demonstrated here, or changes in agonist efficacy, this work provides a careful demonstration of pathway independence and a quantitative assessment of pathway selectivity by each agonist.

It is therefore likely that changes in permeability directly reflect $G_{\alpha_{12/13}}$ activation, and changes in intracellular calcium directly reflect G_{α_q} activation. Hence, the differences observed between thrombin and agonist peptide activation of PAR-1 can be explained by differences in the ability of the receptor to activate $G_{\alpha_{12/13}}$ or G_{α_q} . This hypothesis would imply that agonist peptides induce the receptor to couple differently to its G protein families, suggesting functional selectivity of PAR-1 signaling.

A diverse spectrum of GPCRs has been found to show prop-

erties of functional selectivity. In the human serotonin 2C receptor, for example, it was shown that certain agonists can preferentially activate the PLC/IP₃ pathway, whereas other agonists favored the phospholipase A₂/arachidonic acid release pathway, even though both signal through the same receptor (1). In octopamine/tyramine receptors, studies have shown that activation of the same receptor by two different small molecule agonists differs in their rank order potency to induce two second messenger systems (7).

In general, it has been shown in systems like these, depending on which signaling response is assayed, a single receptor can have different pharmacological profiles. The diversity of receptors that display this type of pharmacology, or functional selectivity, illuminates possible mechanisms that could explain conflicting observations made in PAR-1 signaling.

However, the mechanism by which thrombin activates PAR-1 differently from agonist peptide could be the result of protein/protein interactions of thrombin either directly with the PARs or with other thrombin receptors present on the cell surface which cannot be recapitulated with the short agonist peptides. For example, others have shown in HUVEC that nonproteolytic thrombin promotes cell growth but not intracellular calcium mobilization or monolayer permeability (66). We found, however, that concomitant stimulation with subsaturating concentrations of agonist peptide and catalytically inactivated thrombin had no effect on either calcium mobilization or monolayer permeability (Fig. 4A). These results suggest that after the tethered ligand is enzymatically generated by thrombin further association with the enzyme does not modulate the signaling properties. This conclusion also implies that the functional difference arises from the tethered *versus* free nature of the activating ligand, perhaps from the geometrical constraints placed on the ligand by the covalently attached tethering linker and/or by conformational changes induced allosterically by the linker itself.

The possibility of receptors other than PARs altering the signaling of thrombin *versus* agonist peptide is not likely. Although thrombomodulin is highly expressed in endothelial cells (83–85) and known to bind directly to thrombin, the ability of thrombomodulin to signal on its own is suspect because of its single transmembrane domain and small cytoplasmic tail. It is possible, however, that a thrombin-thrombomodulin complex may allosterically alter the way thrombin interacts with PAR-1. If that were the case, it would support the hypothesis that PAR-1 can be activated in different manners, which affect G protein coupling specificity. However, we show that addition of catalytically inactivated thrombin did not affect subsaturating stimulatory responses to agonist peptide (Fig. 4A), suggesting that a nonproteolytic thrombin protein/protein interaction with PAR-1, thrombomodulin, or other thrombin receptor present on the cell surface does not alter PAR-1-mediated signaling.

In addition to thrombomodulin, activation of MMP-2 by thrombin could present an alternate pathway by which thrombin facilitates monolayer permeability. Proteinases of the extracellular matrix, including MMP-2 and -9, have been linked to thrombin signaling and/or monolayer permeability (70, 71). However, when HMEC-1 were treated with a general MMP inhibitor, it had no effect on subsaturating stimulation by thrombin or TK compared with vehicle control (Fig. 4B). Given that concentrations of agonist used were close to the EC_{50} for either induced barrier permeability or intracellular calcium mobilization, it is reasonable to conclude that a lack of effect at this dose would be reflected in a lack of change in the overall dose response. It is therefore not likely that the observed differences between thrombin and agonist peptide are the result of proteolytic activation of MMP-2 by thrombin and not agonist peptides.

Other differences have been observed when agonist peptides are used to activate PAR-1 (35–39, 86). Some of the most compelling evidence has recently come forth from studies involving site-directed mutagenesis of the PAR-2 receptor. Al-Ani *et al.* (86) showed that mutagenesis of the tethered ligand sequence from SLIGRL to either SLAAA or SAIGRL had little effect on trypsin-mediated receptor signaling. Importantly, however, neither of the free agonist peptides, SLAAA-NH₂ nor SAIGRL-NH₂, showed any activity compared with a peptide of the wild type sequence. These data imply that free agonist peptides can confer different conformational states of receptor activation, an observation that is substantiated by our present work. Our hypothesis that agonist peptides induce different active receptor conformations that lead to alterations in G protein coupling illuminates such observations.

The stabilization of agonist-receptor complexes for different intracellular partner proteins is predicted by the “floating” or “mobile” receptor hypothesis. Originally conceived to describe hormone receptor signaling pre-G protein discovery, this model predicted that both the receptor and the protein with which it directly couples diffuse laterally in the plane of the lipid bilayer (87–89). The differences observed in signaling properties between cell types that express the same receptor could then be explained by differences in the cellular constitution of these coupling proteins. More recently, in light of advances in pharmacology and the advent of the G protein field, a similar model has been put forward to explain how different agonists function through a single receptor with different outcomes, termed ligand-induced functional selectivity. This phenomenon of functional selectivity of receptor signaling has only recently begun to receive due attention. However, because of their unique mode of activation, until now PARs have not been thought of as functionally selective.

The underlying mechanism that allows a single receptor to alter its ability to couple to differential effector pathways remains largely speculative. One possibility is that for each compound/receptor interaction, a unique conformational state in the receptor is stabilized. Each state then has different coupling affinities for the different G proteins. Several groups have shown evidence that substantiates a multiple conformational states model (90–93). It is clear by the current state of the field that this mechanism must be described further.

The mechanisms that could give rise to the observed differences were explored further by performing simulations using a mathematical model that incorporated the current understanding of these two pathways in HMEC-1. Such an extensive mathematical model of two divergent GPCR signaling events from a single receptor has not been attempted previously. The model was initially constructed using experimentally determined kinetic parameters extracted from the literature. Those steps in the cascades whose biochemistry has not been well studied or reported were judiciously fixed so as to set parameters of the model to produce the best fit with the experimentally determined thrombin-induced calcium mobilization data. At all concentrations of thrombin or TK, the peak height correlated highly with the simulations (Fig. 6, A and B). Given that the EC₅₀ for thrombin-induced TER, Rho activation, and the theoretical prediction correlated and were not statistically different (Fig. 6D), this justified the use of mathematically representing Rho activation as a model for barrier permeability.

Initially the relative concentrations of G α_q and G $\alpha_{12/13}$ and the receptor-catalyzed activation efficiencies were mathematically set to be identical for each G protein. Simulations predicted the EC₅₀ for Rho activation to be ~10-fold lower than that of calcium mobilization, which matched that observed experimentally (Fig. 7A). The model revealed that this differ-

ence is primarily the result of the difference in GTPase-activating protein (GAP) activity of the RGS domain of the G α_q GAP, PLC- β , and the G $\alpha_{12/13}$ GAP, p115RhoGEF. p115RhoGEF is a much poorer GAP than PLC- β differing by 300–2,500-fold (23). Taken together with the observation that RGS domains are highly specific for G protein families (94), the consequence is that G $\alpha_{12/13}$ requires less activated receptor than G α_q to be activated. This conclusion implies the threshold for G protein activation is highly dependent upon the mechanisms that negatively oppose the system (95–99). However, the reversal observed for agonist peptide activation was not predicted by the initial model (Fig. 7B).

In the construction of the model, experimentally determined rate constants were used to describe this activation. In the case of agonist peptide, the threshold for receptor activation is dictated solely by the affinity of the agonist peptide for the receptor. When the affinity parameter for agonist peptide and PAR-1 was varied, the EC₅₀ values for both calcium mobilization and induced barrier permeability were shifted in unison (see supplemental figure). Thus, the reversal of EC₅₀ values observed experimentally does not arise simply by differences in the mechanism of receptor activation.

Simulations were performed to search for a set of conditions which could predict the experimental observations. One possible set of conditions altered the ratio of the K_d for the activated receptor-G α_q complex to the K_d for activated receptor-G $\alpha_{12/13}$. When they were set to differ by ~800-fold in favor of G α_q activation, the curves switch activation order and match experimental data well (Fig. 7C).

The results of modeling the two pathways have provided insights into the governing mechanisms of the system that might otherwise have not been duly considered. Predictions such as the dominating influence of the negative signal regulating GAP proteins, although they make sense in hindsight, are brought clearly to the forefront of thinking about these pathways. The repercussions on subsequent signal propagation of receptor activation by enzymatic cleavage compared with that of ligand-binding activation, although overtly different in mechanism, are not readily apparent intuitively or experimentally. Mathematical simulations have allowed us to explore these differences in a straightforward manner.

In fact, the precise means by which the cell senses and responds accordingly to different thrombin concentrations has long been debated. One hypothesis proposed by Ishii *et al.* (100) presented a model in which dose-dependent responses were a result of a balance between opposing events of activation and second messenger clearance. This model predicted each receptor activation event by thrombin would result in a “quantum” of second messenger formation. As a consequence, at low levels of thrombin receptors are continually being activated, until ultimately the entire reserve is depleted. However, at low thrombin concentrations the rate at which they are activated would not out-perform the rate at which second messengers would be cleared. Hence, second messenger levels would not reach critical thresholds above which committed signaling would occur. Our mathematical model confirmed this opposing rate hypothesis. The model revealed the primary difference between enzymatic activation by thrombin *versus* protein/protein interaction activation by agonist peptide sets the threshold for receptor activation and has no effect on the relative activations of the different G proteins themselves or the final outputs of the signaling cascades. In the case of thrombin, the receptor activation threshold is dictated by the rate constants that describe the enzymatic cleavage of the receptor. In addition, the model also revealed that either mechanism of receptor activation would result in dose-dependent calcium responses, suggesting

that the concentration of thrombin is directly reflected in the amount of generated tethered ligand or signaling receptor. Therefore the relative EC₅₀ values for calcium mobilization compared with induced barrier permeability reflect this tethered ligand model of receptor activation. This should then be contrasted with the reversal in EC₅₀ values observed from the free agonist peptide activation experiments. Taken together this would support the hypothesis that the signaling properties of the receptor can be altered intramolecularly by a covalently bound agonist compared with an agonist peptide.

These predictions, however, do not rule out other possibilities such as receptor dimerization and transactivation. We show here that HMEC-1 do not respond to PAR-4 agonist peptides (Fig. 1, A and B), confirming previous reports that indicate that endothelial cells do not express PAR-4 (47). However, there is evidence of PAR-1/PAR-2 heterodimers (15), both of which are expressed in HMEC-1. If thrombin did concomitantly activate both PAR-1 and PAR-2 by transactivation with the tethered ligand of PAR-1, that would likely favor G_{αq} activation given that the PAR-2-specific agonist peptide mobilizes calcium but has no effect on barrier permeability or actin stress fiber formation (Fig. 1). In addition, if one considers the fact that treatment with the PAR-1-specific agonist peptide produced the same results as the nonspecific (PAR-1 and PAR-2) agonist peptide, it is unlikely that PAR-2 plays any significant role in the differences between thrombin and agonist peptide signaling. The possibility of PAR-1/PAR-3 dimerization remains intriguing. However, given that the agonist peptides derived from the tethered ligand of the PAR-3 receptor do not elicit responses via PAR-3 and that the PAR-3 agonist peptides have been shown to activate PAR-1 nonselectively (101), direct testing of this possibility is not straightforward. If, however, PAR-1 did complex with PAR-3, altering signaling properties of PAR-1, this would support the hypothesis that PAR-1 can be activated in different manners which affect G protein coupling specificity.

Others have shown the partial PAR-1 agonist YP to activate platelet shape change without mobilizing calcium stores (52–58). Although there are conflicting results reported in the literature, this effect has been interpreted as preferential activation of G_{α12/13}. In HMEC-1 we found YP to have no effect on induced barrier permeability. These results confirm studies of YP on HUVEC (102, 103).

We demonstrate here that two different agonist peptides activate PAR-1 in a manner that differs from that of thrombin activation. These differences might arise from the fact that the agonist peptide SN, although identical in amino acid sequence, lacks the geometric constraints which are imposed *per force* on the tethered ligand. The distal effects transmitted via the loop that spans between the tethered ligand and the first transmembrane helix are of unknown consequence.

In conclusion, we report here for the first time in an endothelial cell system that activation of PAR-1 with agonist peptides instead of thrombin favors calcium mobilization over induced barrier permeability. Our results suggest that this reflects the ability of PAR-1 to activate G protein subfamilies differentially. This hypothesis implies that the agonist peptide/receptor interaction stabilizes a different conformation of PAR-1 which changes the specificity of the receptor for different G proteins or ligand-induced functional selectivity. This prediction allows for the future exploration of possible agonist peptides which could be engineered to activate or, alternatively, disfavor, the G protein family of choice. Therapeutically, this could be exploited to alter the relative effects of thrombin on the endothelium, minimizing the deleterious bleeding disorders currently associated with anti-thrombin reagents.

Acknowledgments—We thank Laurie Earls for help in confirming the lack of PAR-4 expression in HMEC-1 and Barbara Fingleton and Lynn Matrisian for assistance in determining MMP inhibition. Actin stress fiber formation experiments were performed in part through the use of the Vanderbilt University Medical Center Cell Imaging Shared Resource.

REFERENCES

- Berg, K. A., Maayani, S., Goldfarb, J., Scaramellini, C., Leff, P., and Clarke, W. P. (1998) *Mol. Pharmacol.* **54**, 94–104
- Kurrasch-Orbaugh, D. M., Watts, V. J., Barker, E. L., and Nichols, D. E. (2003) *J. Pharmacol. Exp. Ther.* **304**, 229–237
- Ebersole, B. J., Visiers, I., Weinstein, H., and Sealfon, S. C. (2003) *Mol. Pharmacol.* **63**, 36–43
- Ghanouni, P., Gryczynski, Z., Steenhuis, J. J., Lee, T. W., Farrens, D. L., Lakowicz, J. R., and Kobilka, B. K. (2001) *J. Biol. Chem.* **276**, 24433–24436
- Mottola, D. M., Kiltz, J. D., Lewis, M. M., Connery, H. S., Walker, Q. D., Jones, S. R., Booth, R. G., Hyslop, D. K., Piercey, M., Wightman, R. M., Lawler, C. P., Nichols, D. E., and Mailman, R. B. (2002) *J. Pharmacol. Exp. Ther.* **301**, 1166–1178
- Kiltz, J. D., Connery, H. S., Arrington, E. G., Lewis, M. M., Lawler, C. P., Oxford, G. S., O'Malley, K. L., Todd, R. D., Blake, B. L., Nichols, D. E., and Mailman, R. B. (2002) *J. Pharmacol. Exp. Ther.* **301**, 1179–1189
- Robb, S., Cheek, T. R., Hannan, F. L., Hall, L. M., Midgley, J. M., and Evans, P. D. (1994) *EMBO J.* **13**, 1325–1330
- Kenakin, T. (2004) *Trends Pharmacol. Sci.* **25**, 186–192
- Hermans, E. (2003) *Pharmacol. Ther.* **99**, 25–44
- Andrade-Gordon, P., Derian, C. K., Maryanoff, B. E., Zhang, H. C., Addo, M. F., Cheung, W., Damiano, B. P., D'Andrea, M. R., Darrow, A. L., de Garavilla, L., Eckardt, A. J., Giardino, E. C., Haertlein, B. J., and McCormey, D. F. (2001) *J. Pharmacol. Exp. Ther.* **298**, 34–42
- Hollenberg, M. D., and Saifeddine, M. (2001) *Can. J. Physiol. Pharmacol.* **79**, 439–442
- Nystedt, S., Emilsson, K., Wahlestedt, C., and Sundelin, J. (1994) *Proc. Natl. Acad. Sci. U. S. A.* **91**, 9208–9212
- Hirano, K., and Kanaide, H. (2003) *J. Atheroscler. Thromb.* **10**, 211–225
- Ishihara, H., Connolly, A. J., Zeng, D., Kahn, M. L., Zheng, Y. W., Timmons, C., Tram, T., and Coughlin, S. R. (1997) *Nature* **386**, 502–506
- O'Brien, P. J., Prevost, N., Molino, M., Hollinger, M. K., Woolkalis, M. J., Woulfe, D. S., and Brass, L. F. (2000) *J. Biol. Chem.* **275**, 13502–13509
- Schmidt, V. A., Nierman, W. C., Maglott, D. R., Cupit, L. D., Moskowitz, K. A., Wainer, J. A., and Bahou, W. F. (1998) *J. Biol. Chem.* **273**, 15061–15068
- Nakanishi-Matsui, M., Zheng, Y. W., Sulciner, D. J., Weiss, E. J., Ludeman, M. J., and Coughlin, S. R. (2000) *Nature* **404**, 609–613
- Barr, A. J., Brass, L. F., and Manning, D. R. (1997) *J. Biol. Chem.* **272**, 2223–2229
- Vanhauwe, J. F., Thomas, T. O., Minshall, R. D., Tiruppathi, C., Li, A., Gilchrist, A., Yoon, E. J., Malik, A. B., and Hamm, H. E. (2002) *J. Biol. Chem.* **277**, 34143–34149
- Malik, A. B., and Fenton, J. W., Jr. (1992) *Semin. Thromb. Hemostasis* **18**, 193–199
- Rabiet, M. J., Plantier, J. L., and Dejana, E. (1994) *Br. Med. Bull.* **50**, 936–945
- Rabiet, M. J., Plantier, J. L., Rival, Y., Genoux, Y., Lampugnani, M. G., and Dejana, E. (1996) *Arterioscler. Thromb. Vasc. Biol.* **16**, 488–496
- Kozasa, T., Jiang, X., Hart, M. J., Sternweis, P. M., Singer, W. D., Gilman, A. G., Bollag, G., Sternweis, P. C., Sharma, S., elMasry, N., Qiu, R. G., McCabe, P., and Polakis, P. (1998) *Science* **280**, 2109–2111
- Fukuhara, S., Chikumi, H., and Gutkind, J. S. (2000) *FEBS Lett.* **485**, 183–188
- Fukuhara, S., Murga, C., Zohar, M., Igishi, T., and Gutkind, J. S. (1999) *J. Biol. Chem.* **274**, 5868–5879
- Jackson, M., Song, W., Liu, M. Y., Jin, L., Dykes-Hoberg, M., Lin, C. I., Bowers, W. J., Federoff, H. J., Sternweis, P. C., and Rothstein, J. D. (2001) *Nature* **410**, 89–93
- Wojciak-Stothard, B., and Ridley, A. J. (2002) *Vasc. Pharmacol.* **39**, 187–199
- Tiruppathi, C., Minshall, R. D., Paria, B. C., Vogel, S. M., and Malik, A. B. (2002) *Vasc. Pharmacol.* **39**, 173–185
- Borbiev, T., Verin, A. D., Shi, S., Liu, F., and Garcia, J. G. (2001) *Am. J. Physiol.* **280**, L983–L990
- van Nieuw Amerongen, G. P., van Delft, S., Vermeer, M. A., Collard, J. G., and van Hinsbergh, V. W. (2000) *Circ. Res.* **87**, 335–340
- Bogatcheva, N. V., Garcia, J. G., and Verin, A. D. (2002) *Biochemistry (Mosc.)* **67**, 75–84
- Scarborough, R. M., Naughton, M. A., Teng, W., Hung, D. T., Rose, J., Vu, T. K., Wheaton, V. I., Turck, C. W., and Coughlin, S. R. (1992) *J. Biol. Chem.* **267**, 13146–13149
- Garcia, J. G., Patterson, C., Bahler, C., Aschner, J., Hart, C. M., and English, D. (1993) *J. Cell. Physiol.* **156**, 541–549
- Blackhart, B., Emilsson, K., Nguyen, D., Teng, W., Martelli, A., Nystedt, S., Sundelin, J., and Scarborough, R. (1996) *J. Biol. Chem.* **271**, 16466–16471
- Vouret-Craviari, V., Van Obberghen-Schilling, E., Rasmussen, U. B., Pavirani, A., Lecocq, J. P., and Pouyssegur, J. (1992) *Mol. Biol. Cell* **3**, 95–102
- Vouret-Craviari, V., Van Obberghen-Schilling, E., Scimeca, J. C., Van Obberghen, E., and Pouyssegur, J. (1993) *Biochem. J.* **289**, 209–214
- Blackhart, B. D., Ruslim-Litrus, L., Lu, C. C., Alves, V. L., Teng, W., Scarborough, R. M., Reynolds, E. E., and Oksenberg, D. (2000) *Mol. Pharmacol.* **58**, 1178–1187
- Hollenberg, M. D. (2000) *Mol. Pharmacol.* **58**, 1175–1177
- Al-Ani, B., Wijesuriya, S. J., and Hollenberg, M. D. (2002) *J. Pharmacol. Exp. Ther.* **302**, 1046–1054
- Riewald, M., and Ruf, W. (March, 2005) *J. Biol. Chem.* **10.1074/jbc.M500747200**
- Tiruppathi, C., Malik, A. B., Del Vecchio, P. J., Keese, C. R., and Giaever, I.

- (1992) *Proc. Natl. Acad. Sci. U. S. A.* **89**, 7919–7923
42. McCarthy, S. A., and Bicknell, R. (1992) *J. Biol. Chem.* **267**, 21617–21622
 43. Kim, J. A., Kang, Y. S., Lee, S. H., Lee, E. H., and Lee, Y. S. (2001) *J. Cell. Biochem.* **81**, 93–101
 44. Rajagopalan-Gupta, R. M., Rasenick, M. M., and Hunzicker-Dunn, M. (1997) *Mol. Endocrinol.* **11**, 538–549
 45. Harrell, P. C., McCawley, L. J., Fingleton, B., McIntyre, J. O., and Matrisian, L. M. (2005) *Exp. Cell Res.* **303**, 308–320
 46. Mohammed, F. F., Smookler, D. S., Taylor, S. E., Fingleton, B., Kassiri, Z., Sanchez, O. H., English, J. L., Matrisian, L. M., Au, B., Yeh, W. C., and Khokha, R. (2004) *Nat. Genet.* **36**, 969–977
 47. Ren, X. D., Kiosses, W. B., and Schwartz, M. A. (1999) *EMBO J.* **18**, 578–585
 48. Bohm, S. K., Kong, W., Bromme, D., Smeeckens, S. P., Anderson, D. C., Connolly, A., Kahn, M., Nelken, N. A., Coughlin, S. R., Payan, D. G., and Bunnett, N. W. (1996) *Biochem. J.* **314**, 1009–1016
 49. Hollenberg, M. D., Saifeddine, M., Al-Ani, B., and Kawabata, A. (1997) *Can. J. Physiol. Pharmacol.* **75**, 832–841
 50. Faruqi, T. R., Weiss, E. J., Shapiro, M. J., Huang, W., and Coughlin, S. R. (2000) *J. Biol. Chem.* **275**, 19728–19734
 51. Cupit, L. D., Schmidt, V. A., and Bahou, W. F. (1999) *Trends Cardiovasc. Med.* **9**, 42–48
 52. Rasmussen, U. B., Gachet, C., Schlesinger, Y., Hanau, D., Ohlmann, P., Van Obberghen-Schilling, E., Pouyssegur, J., Cazenave, J. P., and Pavirani, A. (1993) *J. Biol. Chem.* **268**, 14322–14328
 53. Negrescu, E. V., deq Uintana, K. L., and Siess, W. (1995) *J. Biol. Chem.* **270**, 1057–1061
 54. Bauer, M., Retzer, M., Wilde, J. I., Maschberger, P., Essler, M., Aepfelbacher, M., Watson, S. P., and Siess, W. (1999) *Blood* **94**, 1665–1672
 55. Bauer, M., Maschberger, P., Quek, L., Briddon, S. J., Dash, D., Weiss, M., Watson, S. P., and Siess, W. (2001) *Thromb. Haemostasis* **85**, 331–340
 56. Otterdal, K., Pedersen, T. M., and Solum, N. O. (2001) *Thromb. Res.* **103**, 411–420
 57. Dorsam, R. T., Kim, S., Jin, J., and Kunapuli, S. P. (2002) *J. Biol. Chem.* **277**, 47588–47595
 58. Quinton, T. M., Murugappan, S., Kim, S., Jin, J., and Kunapuli, S. P. (2004) *J. Thromb. Haemostasis* **2**, 978–984
 59. Lum, H., and Malik, A. B. (1996) *Can. J. Physiol. Pharmacol.* **74**, 787–800
 60. Gohla, A., Offermanns, S., Wilkie, T. M., and Schultz, G. (1999) *J. Biol. Chem.* **274**, 17901–17907
 61. Hart, M. J., Jiang, X., Kozasa, T., Roscoe, W., Singer, W. D., Gilman, A. G., Sternweis, P. C., Bollag, G., Sternweis, P. M., Sharma, S., elMasry, N., Qiu, R. G., McCabe, P., and Polakis, P. (1998) *Science* **280**, 2112–2114
 62. Cocks, T. M., and Moffatt, J. D. (2000) *Trends Pharmacol. Sci.* **21**, 103–108
 63. Rannels, L. W., and Scarlata, S. F. (1998) *Biochemistry* **37**, 15563–15574
 64. Stam, J. C., Michiels, F., van der Kammen, R. A., Moolenaar, W. H., and Collard, J. G. (1998) *EMBO J.* **17**, 4066–4074
 65. Mehta, D., Ahmed, G. U., Paria, B. C., Holinstat, M., Voyno-Yasenetskaya, T., Tiruppathi, C., Minshall, R. D., and Malik, A. B. (2003) *J. Biol. Chem.* **278**, 33492–33500
 66. Schaeffer, P., Riera, E., Dupuy, E., and Herbert, J. M. (1997) *Biochem. Pharmacol.* **53**, 487–491
 67. Herbert, J. M., Dupuy, E., Laplace, M. C., Zini, J. M., Bar Shavit, R., and Tobelem, G. (1994) *Biochem. J.* **303**, 227–231
 68. Sower, L. E., Payne, D. A., Meyers, R., and Carney, D. H. (1999) *Exp. Cell Res.* **247**, 422–431
 69. Seymour, M. L., Zaidi, N. F., Hollenberg, M. D., and MacNaughton, W. K. (2003) *Am. J. Physiol.* **284**, C1185–C1192
 70. Behzadian, M. A., Wang, X. L., Windsor, L. J., Ghaly, N., and Caldwell, R. B. (2001) *Investig. Ophthalmol. Vis. Sci.* **42**, 853–859
 71. Lafleur, M. A., Hollenberg, M. D., Atkinson, S. J., Knauper, V., Murphy, G., and Edwards, D. R. (2001) *Biochem. J.* **357**, 107–115
 72. Zhong, H., Wade, S. M., Woolf, P. J., Linderman, J. J., Traynor, J. R., and Neuhig, R. R. (2003) *J. Biol. Chem.* **278**, 7278–7284
 73. Hofer, T., Venance, L., and Giaume, C. (2002) *J. Neurosci.* **22**, 4850–4859
 74. De Young, G. W., and Keizer, J. (1992) *Proc. Natl. Acad. Sci. U. S. A.* **89**, 9895–9899
 75. Lemon, G., Gibson, W. G., and Bennett, M. R. (2003) *J. Theor. Biol.* **223**, 93–111
 76. Nystedt, S., Emilsson, K., Larsson, A. K., Strombeck, B., and Sundelin, J. (1995) *Eur. J. Biochem.* **232**, 84–89
 77. Klarenbach, S. W., Chipiuk, A., Nelson, R. C., Hollenberg, M. D., and Murray, A. G. (2003) *Circ. Res.* **92**, 272–278
 78. Stull, J. T., Lin, P. J., Krueger, J. K., Trehwella, J., and Zhi, G. (1998) *Acta Physiol. Scand.* **164**, 471–482
 79. Adelstein, R. S., Conti, M. A., and Pato, M. D. (1980) *Ann. N. Y. Acad. Sci.* **356**, 142–150
 80. Kimura, K., Ito, M., Amano, M., Chihara, K., Fukata, Y., Nakafuku, M., Yamamori, B., Feng, J., Nakano, T., Okawa, K., Iwamatsu, A., and Kaibuchi, K. (1996) *Science* **273**, 245–248
 81. Majumdar, M., Seasholtz, T. M., Goldstein, D., de Lanerolle, P., and Brown, J. H. (1998) *J. Biol. Chem.* **273**, 10099–10106
 82. Majumdar, M., Seasholtz, T. M., Buckmaster, C., Toksoz, D., and Brown, J. H. (1999) *J. Biol. Chem.* **274**, 26815–26821
 83. Preissner, K. T., Nawroth, P. P., and Kanse, S. M. (2000) *J. Pathol.* **190**, 360–372
 84. Lafay, M., Laguna, R., Le Bonniec, B. F., Lasne, D., Aiach, M., and Rendu, F. (1998) *Thromb. Haemostasis* **79**, 848–852
 85. Maruyama, I., and Shigetani, K. (1994) *Rinsho Ketsueki* **35**, 234–237
 86. Al-Ani, B., Hansen, K. K., and Hollenberg, M. D. (2004) *Mol. Pharmacol.* **65**, 149–156
 87. Cuatrecasas, P., and Hollenberg, M. D. (1976) *Adv. Protein Chem.* **30**, 251–451
 88. de Haen, C. (1976) *J. Theor. Biol.* **58**, 383–400
 89. Boeynaems, J. M., and Dumont, J. E. (1977) *Mol. Cell. Endocrinol.* **7**, 33–47
 90. Seifert, R., Wenzel-Seifert, K., Gether, U., and Kobilka, B. K. (2001) *J. Pharmacol. Exp. Ther.* **297**, 1218–1226
 91. Peleg, G., Ghanouni, P., Kobilka, B. K., and Zare, R. N. (2001) *Proc. Natl. Acad. Sci. U. S. A.* **98**, 8469–8474
 92. Swaminath, G., Xiang, Y., Lee, T. W., Steenhuis, J., Parnot, C., and Kobilka, B. K. (2004) *J. Biol. Chem.* **279**, 686–691
 93. Gay, E. A., Urban, J. D., Nichols, D. E., Oxford, G. S., and Mailman, R. B. (2004) *Mol. Pharmacol.* **66**, 97–105
 94. Hains, M. D., Siderovski, D. P., and Harden, T. K. (2004) *Methods Enzymol.* **389**, 71–88
 95. Bhalla, U. S., and Iyengar, R. (2001) *Novartis Found. Symp.* **239**, 4–15, 45–51
 96. Verin, A. D., Patterson, C. E., Day, M. A., and Garcia, J. G. (1995) *Am. J. Physiol.* **269**, L99–L108
 97. Hao, N., Yildirim, N., Wang, Y., Elston, T. C., and Dohlman, H. G. (2003) *J. Biol. Chem.* **278**, 46506–46515
 98. Ishida, A., Shigeri, Y., Taniguchi, T., and Kameshita, I. (2003) *Pharmacol. Ther.* **100**, 291–305
 99. Pitcher, J. A., Freedman, N. J., and Lefkowitz, R. J. (1998) *Annu. Rev. Biochem.* **67**, 653–692
 100. Ishii, K., Hein, L., Kobilka, B., and Coughlin, S. R. (1993) *J. Biol. Chem.* **268**, 9780–9786
 101. Hansen, K. K., Saifeddine, M., and Hollenberg, M. D. (2004) *Immunology* **112**, 183–190
 102. Kruse, H. J., Mayerhofer, C., Siess, W., and Weber, P. C. (1995) *Am. J. Physiol.* **268**, C36–C44
 103. Faraut, B., Barbier, J., Ravel-Chapuis, A., Doyennette, M. A., Jandrot-Perus, M., Verdiere-Sahuque, M., Schaeffer, L., Koenig, J., and Hantai, D. (2003) *J. Cell. Physiol.* **196**, 105–112
 104. Ahn, H.-S., Foster, C., Boykow, G., Arik, L., Smith-Torhan, A., Hesk, D., and Chatterjee, M. (1997) *Mol. Pharmacol.* **51**, 350–356
 105. Parry, M. A., Myles, T., Tschopp, J., and Stone, S. R. (1996) *Biochem. J.* **320**, 335–341
 106. Goldsack, N. R., Chambers, R. C., Dabbagh, K., and Laurent, G. J. (1998) *Int. J. Biochem. Cell Biol.* **30**, 641–646
 107. Biddlecome, G. H., Berstein, G., and Ross, E. M. (1996) *J. Biol. Chem.* **271**, 7999–8007
 108. Mukhopadhyay, S., and Ross, E. M. (1999) *Proc. Natl. Acad. Sci. U. S. A.* **96**, 9539–9544
 109. Ross, E. M., and Wilkie, T. M. (2000) *Annu. Rev. Biochem.* **69**, 795–827
 110. Blank, J., Brattain, K., and Exton, J. (1992) *J. Biol. Chem.* **267**, 23069–23075
 111. Singer, W., Miller, R., and Sternweis, P. (1994) *J. Biol. Chem.* **269**, 19796–19802
 112. Yamamoto, K., Kondo, J., Hishida, T., Teranishi, Y., and Takai, Y. (1988) *J. Biol. Chem.* **263**, 9926–9932
 113. Tiruppathi, C., Lum, H., Andersen, T. T., Fenton, J. W., Jr., and Malik, A. B. (1992) *Am. J. Physiol.* **263**, L595–C601